Secondary-Star Insolation on Exoplanets in Circumbinary Orbits

Reid Sherman

December, 2012

Abstract

Kepler-16b, Kepler-34b, Kepler-35b, and Kepler-47b are transiting circumbinary exoplanets with defined orbits and characteristics (Quarles et al. [2012], Welsh et al. [2012], Kane and Hinkel [2012], Orosz et al. [2012]). Circumbinary planets revolve around the barycenter of two stars, generally a larger, brighter primary star and a smaller, dimmer secondary star. In this paper, *Kepler*- exoplanet atmospheres are modeled as convective with radiative boundaries (Taylor [2010], see Figure 4) to generate two datasets; the first includes the insolation contribution from the secondary star, the second disregards the secondary star. These data quantify the significance of the smaller star on the planet's atmospheric *scale height* and surface temperature. I observed an insignificant difference in the scale height and temperature for Kepler 16b and Kepler 47b. However, feedback mechanisms, which were not modeled iteratively, may accentuate the effects of even slight temperature changes for these two exoplanets. The data show a significant difference in the scale height and temperature for Kepler-34b and Kepler-35b. I infer that since these two systems have binary stars with similar masses, "twin binaries" (Kane and Hinkel [2012]), the insolation effect from the secondary star impacts planet's temperature considerably.

Part I
Introduction

Perhaps with some fascination stemming from the fictional planet Tatooine from *Star Wars*, circumbinary exoplanets are sought-after by both amateur and professional astronomers. Circumbinary refers to the orbital configuration of a binary star system with respect to planet(s) in orbit; the planet "orbits the center-of-mass of a central binary system" (Kane and Hinkel [2012]). Refer to Figure 5 in the Appendix for a graphical representation of a circumbinary orbit. From the perspective of an observer on the planet, there are two sunsets and sunrises a day, assuming there is a surface to stand on! Since larger exoplanets are easier to find, there is a selection bias towards finding gas and ice giants. Transit observations of Kepler-16b, Kepler-34b, Kepler-35b, and Kepler-47b demonstrate circumbinary exoplanets are both tidally stable and detectable (Quarles et al. [2012], Welsh et al. [2012], Kane and Hinkel [2012], Orosz et al. [2012]). This paper investigates the consequences of the insolation contribution from the smaller, dimmer, secondary star on

these *Kepler*- exoplanets. As Venus will testify, the surface temperature of a planet with an atmosphere is significantly higher than its effective temperature due to the greenhouse effect. To take this into account, a simple greenhouse atmosphere is structured into the temperature calculations for these exoplanets.

Part II
Background

To date only a handful of circumbinary exoplanets have been confirmed. They are completely dwarfed by the enormous catalogue of confirmed circumstellar exoplanets. For this paper, I focus on four circumbinary planets: Kepler-16b, Kepler-34b, Kepler-35b, and Kepler-47b; using properties (mass, radius) and orbital parameters (semi-major axis, eccentricity) from Quarles et al. [2012], Welsh et al. [2012], Kane and Hinkel [2012], Orosz et al. [2012]. These exoplanets are used because they are relatively small (Neptune or Saturn mass) and transit at least one of their host stars. Transiting planets are studied in this paper because more of their characteristics are constrainable, e.g., the temperature of Kepler-34b and Kepler-35b over the course of an orbit in Figure 1. Methods of inferring planetary characteristics from transit and radial velocity measurements are discussed in the Appendix section *Planetary Orbit*. Additionally, the HZ for Kepler-34 and Kepler-35 is shown in Figure 5 in the Appendix.

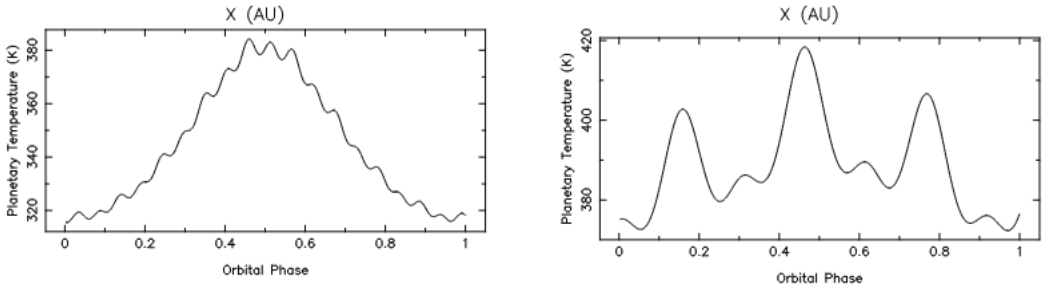

Figure 1: The effective temperature for Kepler-34b (left) and Kepler-35b (right) as a function of orbital position from Kane and Hinkel [2012]. This plot shows the temperature of the exoplanets assuming they have no atmosphere.

Although it is out of this paper's scope, Surface and atmospheric temperature have important ramifications for planetary habitability. A priori, liquid water is essential for all forms of life. The broadest definition of the habitable zone, or HZ, is the region in a extrasolar system where liquid water will not be entirely lost from a planet's surface. If a planet is too hot, it boils away its water and may develop a runaway greenhouse. If a planet is too cold or lacks an atmosphere, it risks freezing away its liquid water. Planetary habitability has been investigated in singular star, or circumstellar, orbits (Kasting et al. [1993], Seager and Deming [2010], Zsom et al. [2012]), as

well as in circumbinary orbits (Kane and Hinkel [2012]). Figure 3 shows the habitable zone for the Solar System, in the left fringe is Venus, a planet that likely experienced a runaway greenhouse in the past. The right fringe is Mars, which likely had its atmosphere stripped away by solar wind and low surface gravity. The exoplanets modeled in this paper are not likely habitable, nor are most in their star's HZ. Circumbinary planet habitability is a niche subtopic of planetary habitability. The reason for this unpopularity may stem from the lack of data. Nonetheless, they are an interesting case in exoplanet astronomy and astrophysics; there are a few publications that discuss circumbinary tidal stability (Doolin and Blundell [2011], Lombardi et al. [2011]) and a recent paper discussing the circumbinary habitable zone (Kane and Hinkel [2012]). Figure 2 from Kane and Hinkel [2012] demonstrates the secondary star may have considerable implications for the habitable zone. In circumbinary systems with secondary stars of comparable size to their primary, the secondary considerably affects the size of the HZ.

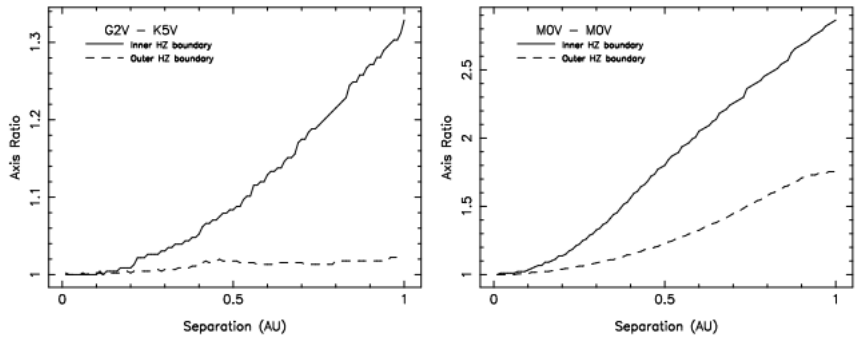

Figure 2: Kane and Hinkel [2012]show the HZ calculations for G2V-K5V and M0V-M0V binary systems. The axis ratio describes the separation between the two stars. An interesting result from Kane and Hinkel [2012] is highly eccentric (> 0.2) circumbinary orbits may move exoplanets in and out of the HZ.

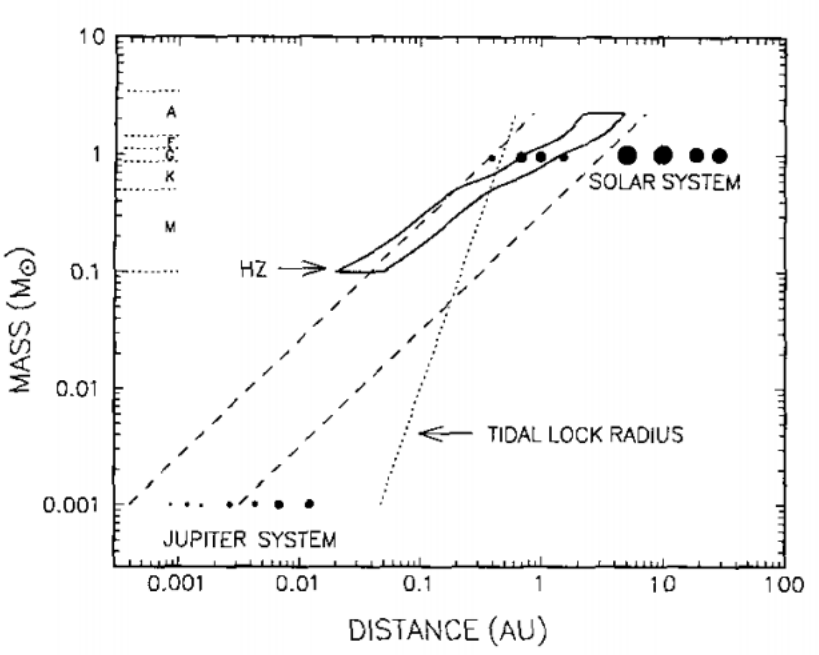

Figure 3: The habitable zone for the Solar System from Kasting et al. [1993].

Part III
Methods

For this paper, exoplanets in stable circumbinary orbits with transit observations and radial velocity measurements are analyzed. In *Planetary Temperature* I structure a convective atmosphere with radiative boundaries for these exoplanets. In *Atmospheric Scale Height*, I derive the scale height from the surface temperature for these exoplanets. The Appendix section *Planetary Orbit* discusses the orbits of circumbinary exoplanets.

1 Planetary Temperature

To calculate the surface temperature of the planet, I assume the two stars are radiative black bodies with emissivity = 1, during non-eclipse. E_0, the combined flux received by the planet, is the sum of the bright and dim star's incident flux, F_1 and F_2, respectively. At the equator, the incoming flux from the binary star system, E_0,

$$E_0 = F_1 + F_2 = \sigma\left(T_1^4\sqrt{\frac{r_1}{a_1}} + T_2^4\sqrt{\frac{r_2}{a_2}}\right) \tag{1}$$

A more sophisticated method of determining the insolation is derived in Kane and Hinkel [2012], which takes into account Wien's law and the peak stellar wavelength emission. For this project, the wavelength of the light emitted from the stars was not taken into account and only their effective temperatures were used. Additionally, if eclipses occur daily or weekly, they may play a small role in the surface temperature calculation. Ignoring limb darkening, $E_0' \approx F_1 - F_2$, where E_0' is the flux at the top of the planet's atmosphere during eclipse. I do not take into account stellar eclipses as they only affect the planet's effective temperature momentarily.

At the top of the atmosphere during non-eclipse,

$$T_{eff} = \sqrt[4]{\frac{E_0(1-\alpha)}{4\sigma}} \equiv \sqrt[4]{\frac{L(1-\alpha)}{16\pi\sigma a^2}} \tag{2}$$

The effective temperature,T_{eff}, is calculable given the average albedo, α, of the planet and the incoming flux from the two stars, E_0, or by using the overall luminosity, L, and the planet's semi-major axis, a. Eccentricity can cause T_{eff} to vary by over 9% from periapse to apsis in certain cases (Orosz et al. [2012]), which is why sophisticated methods would calculate the temperature iteratively. Additionally, the effective temperature calculation tends to underestimate the surface temperature of planets with thick atmospheres like Venus or Earth. Therefore, the following calculations provide a more precise method of estimating the surface temperature (with principles borrowed fromTaylor [2010], and Nimmo [2012]).

In steady state, the received flux from the two stars must equate the outgoing flux,

$$F_{in} = F_{out}$$

Assuming both the star and planet are radiative blackbodies with emissivity = 1, I apply the Stefan-Boltzmann law,

$$\sigma T_{eff}^4 = \sigma T_{eff}^4$$

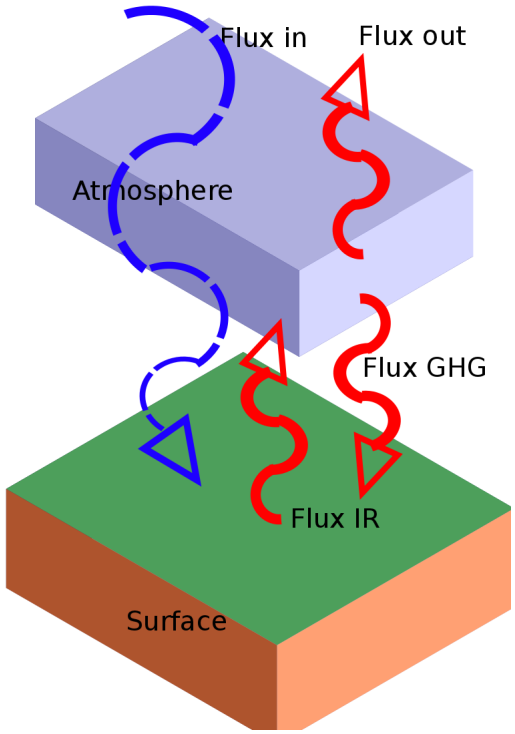

Figure 4: Radiative flux balance to calculate surface temperature. *Flux in* is the shortwave stellar insolation from the star(s), *Flux IR* is the long wave infrared flux emitted from the surface of the exoplanet, *Flux GHG* is the re-emission of longwave infrared flux by greenhouse gasses in the atmosphere, and *Flux out* is the necessary outgoing flux to maintain steady state, i.e., it is equal to *Flux in*. All fluxes are modelled as blackbody radiators with emissivity = 1. To find the surface temperature I apply the Stefan-Boltzmann law, $F = \sigma T^4$, and assume the temperature at the top of the atmosphere is the effective temperature from Equation 2. The atmosphere between the two boundaries (stratosphere and surface) is assumed to move heat through convection.

Assuming the radiative atmosphere from Figure 4 that radiates equally in both directions, the radiating surface infrared flux, $F_{surfaceIR}$, equals,

$$F_{surfaceIR} = 2\sigma T_{eff}^4 \tag{3}$$

The radiating temperature at the surface can be combined with the Stefan-Boltzman equation to calculate the temperature at the surface,T_s,

$$\sigma T_s^4 = 2\sigma T_{eff}^4$$

The flux balance can be rearranged to calculate the surface temperature as a function of the effective temperature,

$$T_s = \sqrt[4]{2} T_{eff} \tag{4}$$

Equation 4 is used to approximate the surface temperature of the exoplanets in *Results and Analysis*.

2 Atmospheric Scale Height

In this section, I analytically derive atmospheric structure by first approximating the *lapse rate* of the transiting exoplanets. The lapse rate describes the temperature change with altitude, which has important meteorological implications. I then infer the scale height, the altitude with surface pressure divided by e, from the lapse rate. The scale height is used as a measure of the importance of the smaller star on the exoplanet's atmospheres. Atmospheric feedbacks that regulate surface temperature are not modeled into the simulated atmospheres. The dry adiabatic lapse rate for the atmosphere is calculable by equating the change in potential energy of a rising packet of air, ΔPE, to its change in temperature, ΔT,

$$\Delta PE = \Delta T$$

Assuming hydrostatic equilibrium and a homogenous atmosphere,

$$-mg\Delta z = mC_p\Delta T$$

After rearranging variables and canceling the masses, the lapse rate, $\frac{\Delta T}{\Delta z}$, is,

$$\frac{\Delta T}{\Delta z} = -\frac{g}{C_p} \tag{5}$$

Equation 4 ignores latent heat released in a moist atmosphere. A wet atmosphere would lower the lapse rate as there would be an extra term in the denominator of Equation 5, i.e., as saturated air rises the water condenses, which releases latent heat into the system. The atmosphere model in this paper ignores air saturation and thus might underestimate the real lapse rate.

For a planet with a convective atmosphere (surrounded by two radiative boundaries, see Figure 4), if the atmospheric temperature is known, then the scale height,H, is calculable using Equation 5,

$$\int_{T_H}^{T_s} dT = -\frac{g}{C_p}\int_0^H dz \tag{6}$$

Solving the definite integral in Equation 6 and rearranging for the scale height, H, as a function of the heat capacity C_p, surface gravity g, and the difference in temperature from the surface to the temperature at H, $T_s - T_H$,

$$H = -\frac{Cp}{g}(T_s - T_H) \tag{7}$$

Except in certain circumstances, there is no accurate way of determining the composition of an exoplanet's atmosphere from transit data. Therefore, the calculated scale heights in *Results and Analysis* are displayed as *per* C_p. Since the atmosphere radiates upwards (Figure 4), its energy flux is the inverse of the surface flux (Nimmo [2012]). Assuming steady state, $F_{in} = F_{out}$,

$$\sigma T_{eff}^4 = 2\sigma T_H^4$$

From the flux balance, the temperature at one scale height is calculable,

$$T_H = \frac{T_{eff}}{\sqrt[4]{2}} \tag{8}$$

The scale height derived in Equation 7 is defined as the exponential-folding pressure of the atmosphere; i.e., the pressure at H is the surface pressure divided by e. Scale height is also calculable using the ideal gas law by setting up a differential equation relating dP with dT, then bounding from the surface pressure P_0 to the scale height pressure $P_0 e^{-1}$. The problem with using the ideal gas law is it assumes constant temperature from the surface to the stratosphere. In the method derived above, the temperature difference is not ignored, but rather "chunked" into a difference. A more sophisticated technique would iteratively step through pressure, temperature, and perhaps even gravity as a function of altitude. This analytical method provides a first-order approach to approximate the scale height with only the planet's effective temperature. The scale height calculation is useful as it allows us to infer certain characteristics of the planet's atmosphere. Table 1 compares the scale height of rocky planets in the Sun's habitable zone, using Equation 7.

Part IV
Results and Analysis

For planets in our solar system, the theoretical scale heights are comparable to the observed values. Table 1 shows scale height calculations for planets in our solar system using principles derived in *Methods*. There is a significant disagreement (80% error!) with the predicted scale height for Venus, which may be attributed to its runaway greenhouse. Methods to account for this disagreement are discussed in the Appendix section *A Sophisticated Climate Model*.

Name	$g(ms^{-1})$	$\Delta T(K)$	$C_p(kJkg^{-1}K^{-1})$	$H_{calc}(km)$	$H_{real}(km)$	H_{err}
Venus	-8.9	110.3	0.709*	8.8	15.9	80%
Earth	-9.8	88.8	1.04	9.1	8.5	6%
Mars	-3.7	75.5	0.709*	14.5	11.1	23%

Table 1: Comparison of scale heights for planets in the Sun's habitable zone (Kasting et al. [1993]) using Equation 7. Earth is assumed to have a pure N_2 atmosphere, whereas Venus and Mars are modeled with CO_2 atmospheres. This table is a sanity check to ensure the physics derived in *Methods* are realistic. T_s and T_H are calculated from the effective temperatures from Williams [2012]: $T_{eff} = \sqrt[4]{\frac{L_\odot(1-\alpha)}{16\pi\sigma a^2}}$, $L_\odot$: solar luminosity, α : albedo, σ: Stefan-Boltzmann constant, a : planet semi-major axis. T_{eff} was then put in 4 and 8 to get the temperature difference between the surface and at a scale height ($T_s - T_H$). The observed scale heights, H_{real}, are from Williams [2012].
*CO_2 atmosphere

3 Exoplanetary Scale Heights and Temperatures

The only unknown in Equation 7 is C_p, the specific heat of the atmosphere. Planets in Table 1 are approximated as having dominantly N_2 or CO_2 based atmospheres. However, the atmospheric compositions for these exoplanets is unknown; in fact, Adams et al. [2008] shows the composition for small exoplanets is indeterminable based on radial velocity measurements and transit detection alone. Since the atmospheric heat capacity, C_p, is speculative for these exoplanets, the scale heights are displayed over C_p. Table 2 shows the input values for the Kepler-16, Kepler-34, Kepler-35, Kepler-47 systems, with data from Quarles et al. [2012], Welsh et al. [2012], Orosz et al. [2012], respectively.

Name	R ($R_\odot$)	T_{eff} (K)	L ($L_\odot$)	a (AU)	g (ms^{-2})
Kepler-16A	0.649	4450	0.15		
Kepler-16B*	0.2026	3600	0.01		
Kepler-16b		208.1		0.7048	-14.52
Kepler-34A	1.1618	5913	1.48		
Kepler-34B	1.0927	5867	1.27		
Kepler-34b		343.8		1.0896	-8.6
Kepler-35A	1.0284	5606	0.94		
Kepler-35B	0.7861	5202	0.41		
Kepler-35b		386.2		0.604	-5.96
Kepler-47A	0.964	5636	0.84		
Kepler-47B	0.3506	3357	0.01		
Kepler-47c		493.0		0.2956	-10.9

Table 2: Extrasolar system Inputs. The surface gravity, g, is calculated from literature values for minimum planetary mass, m, and minimum planetary radius, r, in the equation: $g = \frac{Gm}{r^2}$. For Kepler-47b's surface gravity, however, the 3σ upper-limit mass ($2M_J$) from Orosz et al. [2012] is not used as this created a surface gravity of many hundred Earths; instead a $7M_\oplus$ from a mass-radius relationship is used.
*The star Kepler-16B has not transited the primary star, so neither its temperature nor radius are known. Therefore, I assumed a 1:1 $M_\odot : R_\odot$ relationship.

Name	Surface T_2 (K)	Surface T_1 (K)	ΔT(K)	H_2/C_p (km*)	H_1/C_p (km*)	ΔH (km*)
Kepler-16b	247.5†	245.0	2.5	5.0	5.0	0.0
Kepler-34b	408.9	350.2	58.6	13.9	11.9	2.0
Kepler-35b	459.3	419.8	39.5	22.6	20.6	2.0
Kepler-47b	586.3	583.8	2.4	15.7	15.7	0.0

Table 3: Comparison of calculated scale heights and surface temperatures for circumbinary exoplanets. The subscript 2, e.g., T_2 denotes both the smaller star and the larger star's luminosity is taken into account for the temperature calculation. The subscript 1, e.g., H_1 denotes the secondary star's luminosity was not taken into account for the scale height calculation. The difference in temperature/scale height calculations is denoted by the Δ symbol, i.e., $\Delta H \equiv H_2 - H_1$. A large ΔH or ΔT implies the temperature structure is seriously affected by the smaller star. A small ΔH or ΔT implies the temperature structure of the planet is *not* seriously affected by the smaller star. This ΔT value is different than the ΔT in Table 1, it is not the difference in temperature between the surface and at altitude.
†Kepler-16b is in the star's habitable zone, however, its high surface gravity (14.52 ms^{-2}) makes this planet inhospitable for humans.
*The units are not actually kilometers since the scale height is divided by the heat capacity. This is because heat capacity is unknown for these exoplanets as and indeterminable a priori (Adams et al. [2008]). Since the scale heights are folded by the heat capacity (C_p) they have units of $kmkgK/kJ$, e.g., for Kepler-47b the scale height is 15.7 kilometers if the atmosphere is entirely N_2 (Cp of N_2 is $\approx$ 1 kgK/kJ).

Part V
Conclusion

The temperature calculations displayed in 3 show the secondary star minutely affects Kepler-16b and Kepler-47b (ΔT is 2.5, and 2.4, respectively) and majorly affects Kepler-34b and Kepler-35b. If the extreme temperature fluctuations on Kepler-34b and Kepler-35b shown in Figure 1 from Kane and Hinkel [2012] are caused by the secondary star, this paper should show a high ΔT for these planets. The Kepler-34 and Kepler-35 systems do show fairly high ΔT values (ΔT is 58.6 and 39.5, respectively), thus the secondary star considerably affects the temperatures. Another possibility is that the extreme temperature fluctuations are due to a highly eccentric orbit. However, the literature does not support this claim; Welsh et al. [2012] puts an upper limit of 0.049 on Kepler-35b's eccentricity. Therefore, it the secondary star must have a considerable effect on the exoplanet's surface temperature.

The purpose of this paper is to identify if the star has a considerable effect on the surface temperature of circumbinary extrasolar systems. The data show two systems in which the secondary star significantly effects the surface temperature (Kepler-34 and Kepler-35) and two where its effects

are negligible (Kepler-16 and Kepler-47). I conclude that since three-body systems are chaotic and can vary in infinitely many ways, circumbinary extrasolar systems must be studied in a case-by-case basis.

Appendix

4 Planetary Orbit

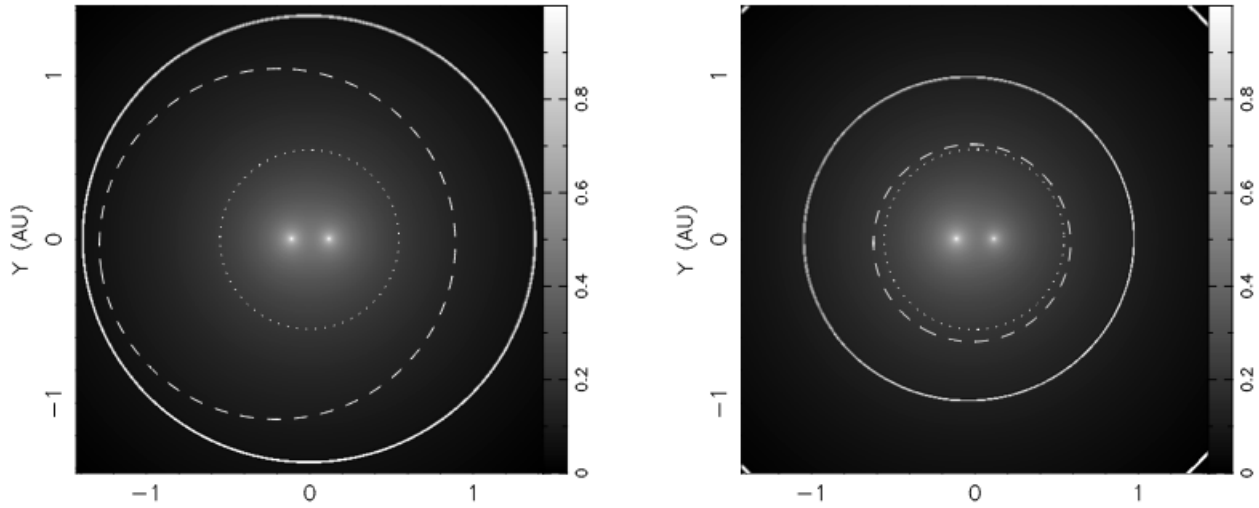

Figure 5: From Kane and Hinkel [2012], Orbital Configuration of Kepler-34 (left) and Kepler-35 (right). The dashed line is the planet's orbit, the solid line is one HZ, the dotten line is the "critical semi-major axis boundary" (basically a lower-limit on stable orbits for particles in circumbinary orbits around these stars, see Doolin and Blundell [2011]).

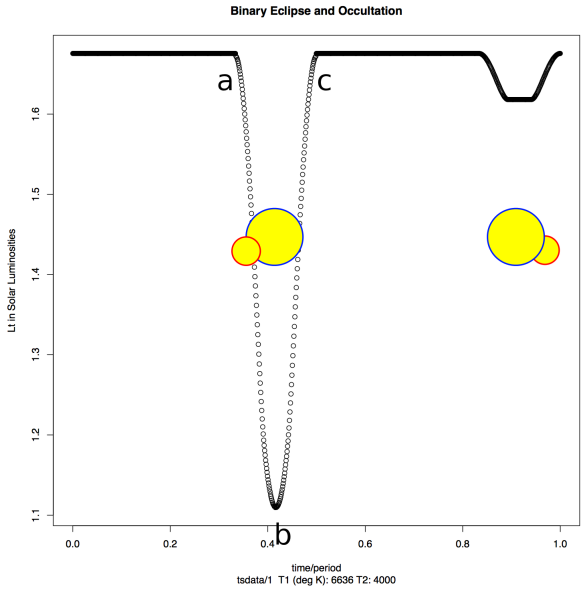

Figure 6: Light curve of an eclipsing binary star system from a modified version of *TwoStars* (Carroll and Ostlie [1996], a computer routine), annotated to show the configuration of the eclipsing stars. The Van Hamme limb darkening equation from Carroll and Ostlie [1996] is used to calculate the flux around t_a and t_c of the eclipse.

Eclipsing stars constrain the star radius very effectively shown in 6. However, the total mass of the binary star system is required to calculate the semi-major axis of the transiting exoplanet. For a binary star system in an eclipsing configuration, the mass is calculable given the inclination i, the period P, and the distance from the observer d. Carroll and Ostlie [1996] derive M_{tot}, the total mass of the binary system,

$$M_{tot} = \frac{4\pi^2}{G}\frac{d}{cos(i)}^3\frac{\alpha^3}{P^2} \tag{9}$$

Where α is the sum of the semi-major axes to the center of mass, i.e., $\alpha = a_1 + a_2$.

The radii of the small star and large star, $r_s$and $r_l$respectively, in an eclipsing configuration are calculable if the system's radial velocity,v, is known.

$$r_s = \frac{v(t_b - t_a)}{2} \tag{10}$$

$$r_l = \frac{v(t_c - t_a)}{2} \tag{11}$$

The times t_a,t_b,and t_c are shown in Figure 6. Intriguingly, an occultation can also be used to constrain the radii in the absence of an eclipse. However, the entry and exit times, t_a and t_c

respectively, will be poorly constrained unless the secondary star is extremely hot. From these radii, entry/exit times, and star masses various orbital properties and planetary/star characteristics are determinable.

5 A Sophisticated Climate Model

The purpose of this section is to discuss how a proper climate model may be used to better approximate the surface temperature and scale height values from this paper. Table 1 in *Results and Analysis* shows there is significant disagreement in the calculated scale height to those observed in the Solar System. The temperature calculation used in this project is too simplistic to conclusively determine exoplanetary surface temperatures. More sophisticated exoplanet climate models take into account feedback mechanisms from chemical processes (Kasting et al. [1993]), iterative atmospheric pressure-temperature structures (Seager and Deming [2010]), and utilize "one-dimensional microphysical cloud models" (Zsom et al. [2012]). Kasting et al. [1993] derives a schematic of feedback mechanisms called the Urey Cycle. The Urey Cycle is an important mechanism for the sequestration of CO_2, an important greenhouse gas. It requires both oceans and ocean life, so Earth is the only known planet known where this reaction occurs.

The following feedback mechanism from Kasting et al. [1993] is for circumstellar orbits, in principle it should also work for circumbinary orbits. Weathering causes calcium carbonate to disassociate into calcium and carbonic acid in the reaction,

$$CaSiO_3 + 2CO_2 \rightarrow Ca^{2+} + 2HCO_3^- + SiO_2 \tag{12}$$

Microscopic organisms use this disassociated calcium in the following biogeochemical reaction,

$$Ca^{2+} + 2HCO_3 \rightarrow CaCO_3 + CO_2 + H_2O$$

The sum of these two equations is the Urey Cycle, which is the process in which CO_2 is transferred into the lithosphere. In the ocean,

$$CaSiO_3 + CO_2 \rightarrow CaCO_3 + SiO_2 \tag{13}$$

The flux of carbon dioxide into silicates is both temperature regulating and temperature regulated. In effect, a slight increase in temperature will increase the rate of weathering, driving Equation 12 forward, lowering atmospheric $[CO_2]$. Consequently, this lowers the planet's surface temperature. As temperature drops, Equation 13 stops moving forward. However, if the temperature drops sufficiently low, runaway cooling may occur, which can theoretically cause global glaciation.

References

E. R. Adams, S. Seager, and L. Elkins-Tanton. Ocean Planet or Thick Atmosphere: On the Mass-Radius Relationship for Solid Exoplanets with Massive Atmospheres. *apj*, 673:1160–1164, February 2008. doi: 10.1086/524925.

B. W. Carroll and D. A. Ostlie. *An Introduction to Modern Astrophysics*. 1996.

S. Doolin and K. M. Blundell. The dynamics and stability of circumbinary orbits. 418:2656–2668, December 2011. doi: 10.1111/j.1365-2966.2011.19657.x.

S. R. Kane and N. R. Hinkel. On the Habitable Zones of Circumbinary Planetary Systems. *ArXiv e-prints*, November 2012.

James F. Kasting, Daniel P. Whitmire, and Ray T. Reynolds. Habitable zones around main sequence stars. *Icarus*, 101(1):108 – 128, 1993. ISSN 0019-1035. doi: 10.1006/icar.1993.1010. URL `http://www.sciencedirect.com/science/article/pii/S0019103583710109`.

J. C. Lombardi, Jr., W. Holtzman, K. L. Dooley, K. Gearity, V. Kalogera, and F. A. Rasio. Twin Binaries: Studies of Stability, Mass Transfer, and Coalescence. 737:49, August 2011. doi: 10.1088/0004-637X/737/2/49.

F. Nimmo. Energy budget, 2012. Lecture Notes.

J. A. Orosz, W. F. Welsh, J. A. Carter, D. C. Fabrycky, W. D. Cochran, M. Endl, E. B. Ford, N. Haghighipour, P. J. MacQueen, T. Mazeh, R. Sanchis-Ojeda, D. R. Short, G. Torres, E. Agol, L. A. Buchhave, L. R. Doyle, H. Isaacson, J. J. Lissauer, G. W. Marcy, A. Shporer, G. Windmiller, T. Barclay, A. P. Boss, B. D. Clarke, J. Fortney, J. C. Geary, M. J. Holman, D. Huber, J. M. Jenkins, K. Kinemuchi, E. Kruse, D. Ragozzine, D. Sasselov, M. Still, P. Tenenbaum, K. Uddin, J. N. Winn, D. G. Koch, and W. J. Borucki. Kepler-47: A Transiting Circumbinary Multiplanet System. *Science*, 337:1511–, September 2012. doi: 10.1126/science.1228380.

B. Quarles, Z. E. Musielak, and M. Cuntz. Habitability of Earth-mass Planets and Moons in the Kepler-16 System. *apj*, 750:14, May 2012. doi: 10.1088/0004-637X/750/1/14.

S. Seager and D. Deming. Exoplanet Atmospheres. 48:631–672, September 2010. doi: 10.1146/annurev-astro-081309-130837.

F.W. Taylor. *Planetary Atmospheres*. Oxford University Press, 2010. ISBN 9780199547418. URL `http://books.google.com/books?id=3sBApwAACAAJ`.

W. F. Welsh, J. A. Orosz, J. A. Carter, D. C. Fabrycky, E. B. Ford, J. J. Lissauer, A. Prša, S. N. Quinn, D. Ragozzine, D. R. Short, G. Torres, J. N. Winn, L. R. Doyle, T. Barclay, N. Batalha, S. Bloemen, E. Brugamyer, L. A. Buchhave, C. Caldwell, D. A. Caldwell, J. L. Christiansen, D. R. Ciardi, W. D. Cochran, M. Endl, J. J. Fortney, T. N. Gautier, III, R. L. Gilliland, M. R.

Haas, J. R. Hall, M. J. Holman, A. W. Howard, S. B. Howell, H. Isaacson, J. M. Jenkins, T. C. Klaus, D. W. Latham, J. Li, G. W. Marcy, T. Mazeh, E. V. Quintana, P. Robertson, A. Shporer, J. H. Steffen, G. Windmiller, D. G. Koch, and W. J. Borucki. Transiting circumbinary planets Kepler-34 b and Kepler-35 b. *nat*, 481:475–479, January 2012. doi: 10.1038/nature10768.

Williams. Planetary fact sheet - metric, September 2012. URL `http://nssdc.gsfc.nasa.gov/planetary/factsheet/`.

A. Zsom, L. Kaltenegger, and C. Goldblatt. A 1D microphysical cloud model for Earth, and Earth-like exoplanets. Liquid water and water ice clouds in the convective troposphere. *ArXiv e-prints*, August 2012.